



Published in final edited form as:

Mol Cancer Ther. 2019 November ; 18(11): 2063–2073. doi:10.1158/1535-7163.MCT-19-0520.

PARP1 Inhibition Radiosensitizes Models of Inflammatory Breast Cancer to Ionizing Radiation

Anna R. Michmerhuizen^{1,2,†}, Andrea M. Pesch^{1,3,†}, Leah Moubadder¹, Benjamin C. Chandler^{1,4}, Kari Wilder-Romans¹, Meleah Cameron¹, Eric Olsen¹, Dafydd G. Thomas^{5,6}, Amanda Zhang¹, Nicole Hirsh¹, Cassandra L. Ritter¹, Meilan Liu¹, Shyam Nyati¹, Lori J. Pierce^{1,5}, Reshma Jagsi^{1,7}, Corey Speers^{1,5,*}

¹Department of Radiation Oncology, University of Michigan, Ann Arbor, MI,

²Program in Cellular and Molecular Biology, University of Michigan,

³Department of Pharmacology, University of Michigan,

⁴Cancer Biology Program, University of Michigan,

⁵Rogel Cancer Center, University of Michigan,

⁶Department of Pathology, University of Michigan,

⁷Center for Bioethics and Social Sciences, University of Michigan.

Abstract

Sustained locoregional control of disease is a significant issue in patients with inflammatory breast cancer (IBC), with local control rates of 80% or less at 5 years. Given the unsatisfactory outcomes for these patients, there is a clear need for intensification of local therapy, including radiation. Inhibition of the DNA repair protein poly adenosine diphosphate-ribose polymerase 1 (PARP1) has had little efficacy as a single agent in breast cancer outside of studies restricted to patients with BRCA mutations; however, PARP1 inhibition (PARPi) may lead to the radiosensitization of aggressive tumor types. Thus, this study investigates inhibition of PARP1 as a novel and promising radiosensitization strategy in IBC. In all existing IBC models (SUM-149, SUM-190, MDA-IBC-3), PARPi (AZD2281-olaparib and ABT-888-veliparib) had limited single agent efficacy (IC₅₀ > 10 μM) in proliferation assays. Despite limited single agent efficacy, sub-micromolar

*Address correspondence to: Corey Speers, M.D., Ph.D., Department of Radiation Oncology, University of Michigan, UH B2 C490, 1500 E. Medical Center Dr., SPC 5010, Ann Arbor, MI 48109-5010, Phone: 734-936-4300, Fax: 734-763-7371, cspeers@med.umich.edu.

Authors' Contributions

Conception and design: A. Michmerhuizen, A. Pesch, L. Moubadder, R. Jagsi, C. Speers

Development and methodology: A. Michmerhuizen, A. Pesch, L. Moubadder, C. Speers

Acquisition of data: A. Michmerhuizen, A. Pesch, L. Moubadder, B. Chandler, K. Wilder-Romans, M. Cameron, E. Olsen, D. Thomas, A. Zhang, N. Hirsh, C. Ritter, M. Liu

Analysis and interpretation of data: A. Michmerhuizen, A. Pesch, L. Moubadder, B. Chandler, K. Wilder-Romans, D. Thomas, M. Liu, S. Nyati, R. Jagsi, C. Speers

Writing, review and/or revision of manuscript: A. Michmerhuizen, A. Pesch, L. Moubadder, B. Chandler, K. Wilder-Romans, M. Cameron, E. Olsen, D. Thomas, A. Zhang, N. Hirsh, C. Ritter, M. Liu, S. Nyati, L. Pierce, R. Jagsi, C. Speers

Administrative, technical, or material support: A. Michmerhuizen, A. Pesch, L. Pierce, R. Jagsi, C. Speers

Study Supervision: R. Jagsi, C. Speers

†these authors contributed equally as shared first authors.

Disclosure of Potential Conflicts of Interest: The authors have no relevant conflicts of interest.

concentrations of AZD2281 in combination with RT led to significant radiosensitization (rER 1.12–1.76). This effect was partially dependent on *BRCA1* mutational status. Radiosensitization was due, at least in part, to delayed resolution of double strand DNA breaks as measured by multiple assays. Using a SUM-190 xenograft model *in vivo*, the combination of PARPi and RT significantly delays tumor doubling and tripling times compared to PARPi or RT alone with limited toxicity. This study demonstrates that PARPi improves the effectiveness of radiotherapy in IBC models and provides the preclinical rationale for the opening phase II randomized trial of RT +/- PARPi in women with IBC (SWOG 1706,).

Keywords

inflammatory breast cancer; radiation sensitivity; PARP inhibitor

Introduction

Inflammatory breast cancer (IBC) diagnoses represent well under 5% of new breast cancer cases but account for a disproportionate share of breast cancer mortality(1). Despite aggressive, multimodal therapy, patients have high rates of locoregional recurrence and distant metastases(1). Treatment strategies for many breast cancer subtypes are largely directed against the protein drivers of each molecular subtype, including targeted therapies against the estrogen receptor (ER) or the human epidermal growth factor receptor 2 (HER2). IBC, however, represents a heterogeneous population that includes tumors across all of the molecular subtypes(2). Current treatment guidelines for IBC patients take into consideration the molecular subtype of the tumor and include anti-HER2 or anti-estrogen therapy when appropriate, but more effective and targeted therapeutic options for patients with IBC are extremely limited. Without more effective alternatives, IBC patients typically receive neoadjuvant chemotherapy followed by mastectomy and adjuvant radiation (RT) to the chest wall and regional lymphatics(1). The key molecular drivers of IBC are currently unknown, and this uncertainty manifests as ineffective clinical therapeutic strategies. In IBC, there is a critical need to identify more effective treatment strategies to decrease rates of locoregional recurrence.

In an attempt to understand the heterogeneity of IBC, a recent study of 53 IBC tumors demonstrated that over 90% of tumors studied contained actionable mutations in genes like *PIK3CA* and *BRCA1/2* that could be targeted using therapies that are either FDA-approved or currently in clinical trial(3). In line with this finding, there are a number of phase I and phase II clinical trials seeking to repurpose other FDA-approved drugs for indication in IBC(1). Targeted therapies in these trials include agents against PD-1 (pembrolizumab), VEGF-A (bevacizumab)(4,5), JAK1/2 (ruxolitinib), and the viral agent T-VEC (talimogene laherparepvec)(1). Many different chemotherapy and radiation therapy regimens have been explored in IBC, but rates of recurrence and overall survival have not significantly improved(6). However, the ability to sensitize IBC tumors to current treatments like radiation represents a promising treatment strategy for patients with IBC.

Inhibition of poly adenosine diphosphate-ribose polymerase 1 (PARP1) has been explored in clinical trials for many cancer types. PARP1 inhibition (PARPi) does not demonstrate significant single agent efficacy in the treatment of most breast cancers(7)-(8); however, PARPi is an effective targeted therapy in subsets of patients harboring *BRCA1/2* mutations(9). In addition to the use of PARP1 inhibitors as monotherapy, our group has shown previously that PARPi can effectively radiosensitize a large range of breast cancer cell lines, including those with functional BRCA1 and BRCA2(10). PARP1, through the addition of poly-ADP ribose (PAR) moieties to sites of single strand DNA (ssDNA) damage, plays a critical role in recognition and recruitment of DNA repair machinery for a variety of different DNA repair processes. If ssDNA lesions go unrepaired, double strand DNA (dsDNA) breaks form. For cells with intact repair pathways, non-homologous end joining (NHEJ) or homologous recombination (HR) allows the cell to repair DNA. In the case of cancers with *BRCA1/2* mutations, where BRCA-mediated homologous recombination is already deficient, the use of PARP1 inhibitors alone can promote the lethal accumulation of dsDNA breaks, leading to selective death of tumor cells – a concept referred to as synthetic lethality. In cells with wild type BRCA, other deficiencies in DNA repair pathways – and the addition of PARPi – may predispose tumor cells to higher levels of DNA damage caused by therapeutic radiation(10). To that end, the present study aimed to determine the effect and efficacy of combining PARP1 inhibition and radiation in multiple preclinical models of IBC.

Materials and Methods

Cell Culture

All IBC cell lines were grown in HAMS F12 media (Gibco 11765–054) in a 5% CO₂ incubator. Media for SUM-149 cells was supplemented with 5% FBS (Atlanta Biologicals), 10mM HEPES (Thermo Fisher 15630080), 1x antibiotic-antimycotic (anti-anti, Thermo Fisher 15240062), 1µg/mL hydrocortisone (Sigma H4001), and 5µg/mL insulin (Sigma I9278). SUM-190 media was supplemented with 1% FBS, 1µg/mL hydrocortisone, 5µg/mL insulin (Sigma I0516), 50nM sodium selenite (Sigma S9133), 5µg/mL apo-Transferrin (Sigma T-8158), 10nM triiodo thyronine (T3, Sigma T5516), 10mM HEPES, and 0.03% ethanolamine (Sigma 411000). MDA-IBC-3 cells were grown with 10% FBS, 1µg/mL hydrocortisone, 1x anti-anti, and 5µg/mL insulin (Sigma I0516). SUM cell lines were obtained from Stephen Ethier at the Medical University of South Carolina, and MDA-IBC-3 cells were obtained directly from Wendy Woodward at the University of Texas MD Anderson Cancer Center. All cell lines were routinely tested for mycoplasma contamination (Lonza LT07–418) and were authenticated using fragment analysis at the University of Michigan DNA sequencing core. Olaparib (MedChem Express HY-10162) and veliparib (MedChem Express HY-10129) were reconstituted in 100% DMSO for cellular assays.

Proliferation Assays

SUM-190 and SUM-149 cells were plated in 96 well plates overnight and treated the next morning with either olaparib or veliparib using a dose range of 1pM to 10µM. After 72 hours, AlamarBlue (Thermo Fisher DAL1025) was added up to 10% of the final volume and read on a microplate reader after incubation at 37°C for 3 hours. MDA-IBC-3 cells were

plated in 6-well plates and treated with a dose range of 1nM to 10 μ M of either olaparib or veliparib. After 72 hours, cells were trypsinized and counted with a hemocytometer.

Clonogenic Survival Assays

SUM-149 and SUM-190 cells were plated at various densities from single cell suspension in 6-well plates and radiated the following day after a one-hour pretreatment with olaparib. Cells were grown for up to three weeks, then fixed with methanol/acetic acid and stained with 1% crystal violet. Colonies with a minimum of 50 cells were counted for each treatment condition. Plating efficiency was determined and used to calculate toxicity. Cell survival curves were calculated as described previously(10). MDA-IBC-3 cells were grown in soft agar (Thermo Fisher 214050) with a base layer of 0.5% agar solution and a top layer of 0.4% agar containing the cell suspension. Drug treatments in supernatant media were added fresh each week. Colonies were grown for up to four weeks before staining with 0.005% crystal violet.

Immunofluorescence

Cells were plated on 18 mm coverslips in 12-well plates and allowed to adhere to coverslips overnight. The following day, cells were treated with media containing either olaparib or vehicle one hour before radiation (2 Gy), and coverslips were fixed at predetermined time points after radiation. γ H2AX foci were detected using anti-phospho-histone H2AX (ser139) monoclonal antibody (Millipore 05–636), with a goat anti-mouse fluorescent secondary antibody (Invitrogen A11005). At least 100 cells were scored visually for γ H2AX foci in three independent experiments. Cells containing ≥ 15 γ H2AX foci were scored positive and were pooled for statistical analysis.

Immunoblotting

Cells were plated overnight and pre-treated the next morning with olaparib. Plates were irradiated one hour after pretreatment, and cells were harvested at 6 and 24 hours after radiation. Lysates were extracted using RIPA buffer (Thermo Fisher 89901) containing protease and phosphatase inhibitors (Sigma-Aldrich PHOSS-RO, CO-RO). Proteins were detected using the anti-PAR antibody (LS-B12794, 1:5000), the anti-PARP1 antibody (ab6079, 1:1000), and anti- β -Actin (8H10D10, Cell Signaling 12262S, 1:50,000).

Xenograft Models

Bilateral subcutaneous flank injections were performed on 4–6 week old CB17-SCID female mice with 1×10^6 SUM-190 cells resuspended in 100 μ L PBS with 50% Matrigel (Thermo Fisher CB-40234). Tumors were allowed to grow until reaching approximately 80mm³. Olaparib treatment was given by intraperitoneal injection 24 hours prior to the first radiation treatment. For long term studies, mice were treated with vehicle (10% 2-hydroxypropyl-beta-cyclodextrin in phosphate buffered saline, Thermo Fisher 10010–023), olaparib (50mg/kg) alone, radiation alone (2 Gy \times 8 fractions) or the combination of olaparib + RT, with 16–20 tumors per treatment group. Tumor growth was measured three times a week using digital calipers, and mice were weighed on the same days. Tumor volume was calculated using the equation $V=(L*W^2)*\pi/6$. For short term studies, mice were treated with

vehicle control, olaparib, or radiation for 48 hours before the tumors were harvested. Mice treated with both olaparib and radiation received olaparib treatment 24 hours before radiation treatment. The tumors were then harvested 48 hours after radiation. Immunohistochemical staining was performed on tumors for all four conditions. All procedures involving mice were approved by the Institutional Animal Care & Use Committee (IACUC) at the University of Michigan and conform to their relevant regulatory standards.

Irradiation

Irradiation was carried out using a Philips RT250 (Kimtron Medical) at a dose rate of approximately 2 Gy/min in the University of Michigan Experimental Irradiation Core as previously described(10). Irradiation of mouse tumors was carried out as described previously(11).

Immunohistochemistry

Immunohistochemical staining was performed on the DAKO Autostainer (Agilent, Carpinteria, CA) using Envision+ or liquid streptavidin-biotin and diaminobenzadine (DAB) as the chromogen. De-paraffinized sections were labeled with the antibodies listed in Supplemental Table 1 for 30 minutes at ambient temperature. Microwave epitope retrieval, as specified in Supplemental Table 1, was used prior to staining for all antibodies. Appropriate negative (no primary antibody) and positive controls (as listed in Supplemental Table 1) were stained in parallel with each set of slides studied. Whole-slide digital images were generated using an Aperio AT2 scanner (Leica Biosystems Imaging, Vista, CA, USA) at 20X magnification, with a resolution of 0.5 μm per pixel. The scanner uses a 20x / 0.75 NA objective and an LED light source. The same instrument and settings were used throughout the study for all whole-slide images generated. The images were checked for quality before use, and scans were repeated as necessary. Digital slides were analyzed using the Visopharm image analysis software suite (DK-2970 Hoersholm, Denmark, v2019.2) to count stained and unstained nuclei.

Comet Assay

Cells were plated in 6 well plates and allowed to adhere overnight. Cells were pretreated with olaparib for one hour before radiation and collected at designated time points after radiation. Cells were mixed with low melting point agarose (Thermo Fisher 15-455-200) and spread on CometSlides (Trevigen 4250-050-03). The cells were lysed with lysis solution (Trevigen 4250-050-01), and DNA was separated by electrophoresis. Propidium iodide (Thermo Fisher P3566) was used to stain DNA. A fluorescent microscope was used to take images of at least 50 cells/treatment. Images were analyzed using Comet Assay IV Software Version 4.3 to calculate the Olive tail moment. Results were pooled for statistical analyses.

Statistical Analyses

GraphPad Prism 7.0 was used to perform statistical tests. *In vitro* statistical analyses were performed using the two-tailed student's t-test or a one-way ANOVA in the case of multiple

comparisons. For *in vivo* studies, a two way ANOVA was used to compare tumor growth, and the fractional tumor volume (FTV) method for assessing synergy *in vivo* was used as previously described(12,13).

Results

Single agent PARPi does not significantly affect proliferation of IBC cell lines *in vitro*

First, we sought to characterize the effect of two PARP1 inhibitors, olaparib (AZD2281) and veliparib (ABT-888) (14), on the proliferation of IBC cell lines. In SUM-190 and MDA-IBC-3 cells, single agent PARPi with olaparib or veliparib does not cause a significant decrease in proliferation at concentrations up to 10 μ M (Fig. 1A–D). While veliparib does not appear to impact proliferation of SUM-149 cells (IC₅₀ > 10 μ M, Fig. 1E), olaparib does have a modest effect as a single agent in SUM-149 cells (IC₅₀ = 2.2 μ M, Fig. 1F). All models tested were isolated from patients with IBC; however, SUM-149 cells are unique as they harbor a *BRCA1* 2288delT mutation as well as allelic loss of the wild type *BRCA1* gene, rendering them BRCA1 deficient(15). Thus, SUM-149 cells may be especially sensitive to additional inhibition of DNA repair pathways(15).

PARPi leads to radiosensitization of IBC cell lines *in vitro*

While single agent PARPi with either olaparib or veliparib did not inhibit cell proliferation, we sought to determine the effect of PARP1 inhibition on the radiosensitivity of IBC cell lines. Clonogenic survival assays were performed with olaparib in each of the three IBC cell lines, as olaparib is a more potent PARP1 inhibitor compared to veliparib, with both PARP1 enzymatic inhibition efficacy and PARP trapping function. All IBC cell lines displayed significant radiosensitization as a result of pretreatment with olaparib. In SUM-190 cells, a dose-dependent radiosensitization was observed, with average radiation enhancement ratios (rER) of 1.45 ± 0.03 and 1.64 ± 0.21 at concentrations of 1 μ M and 2 μ M olaparib, respectively (Fig. 2A, Supplemental Fig. 1A). A similar trend was observed in MDA-IBC-3 cells, with enhancement ratios of 1.12 ± 0.08 and 1.28 ± 0.06 under the same treatment conditions (Fig. 2C, Supplemental Fig. 1B). Because SUM-149 cells express a truncated form of the BRCA1 protein, treatment with olaparib leads to marked radiosensitization at much lower doses. At 10nM and 20nM, the average enhancement ratios for SUM-149 cells were approximately 1.42 ± 0.01 and 1.76 ± 0.11 (Fig. 2E, Supplemental Fig. 1C). The enhancement ratios observed here are similar to or greater than that of cisplatin (rER=1.2–1.3), a compound well-characterized for its ability to act as a radiosensitizing agent(16),(17). Furthermore, the surviving fraction of cells at 6 Gy (Fig. 2B, 2D, 2F) was significantly lower across all three inflammatory cell lines with the addition of olaparib. The radiation enhancement ratios demonstrated a marked dose-dependent increase, while toxicity from each treatment was minimal (Supplemental Fig. 1).

PARP1 inhibition and radiation leads to delayed repair of DNA double strand breaks compared to radiation alone

In cancer cells, ionizing radiation induces both single strand and double strand DNA breaks. In situations where DNA repair is inhibited and single strand breaks go unrepaired, the collapse of replication forks can propagate chromosomal damage and lead to the

accumulation of lethal dsDNA breaks. Because PARP1 is involved in the recruitment of DNA repair proteins to DNA strand breaks, we sought to understand the effect of PARP1 inhibition and radiation on the accumulation of DNA damage in IBC cell lines. In SUM-190 and SUM-149 cells, radiation treatment alone (2 Gy) induces γ H2AX foci in greater than 75% of cells (Fig. 3A,B). In both cell lines, dsDNA breaks are retained at significantly higher levels at 12 and 16 hours after treatment with olaparib and radiation compared to treatment with radiation alone (Fig. 3C,D). Furthermore, a similar difference in dsDNA breaks was observed between RT alone and combination treatment in SUM-190 cells at 4 hours after radiation. In short, the presence of olaparib leads to the accumulation and persistence of dsDNA breaks in the combination treatment compared to the radiation treatment alone in both SUM-190 and SUM-149 cells. In order to independently confirm these findings, we performed the neutral comet assay to assess for dsDNA breaks (Fig. 4A). In SUM-190 cells, the combination of PARPi and RT in SUM-190 cells lead to a significantly longer tail moment, indicating increased dsDNA breaks compared to treatment with RT alone ($p = 0.029$). The tail moment was also significantly higher compared to cells treated with vehicle or olaparib as a single agent (Fig. 4A). Representative images for each treatment condition are shown (Fig. 4A).

Olaparib effectively inhibits PAR formation in IBC cell lines

In order to determine if inhibition of PARP1 enzymatic activity occurs at concentrations of olaparib that are sufficient to induce radiosensitization, we treated cells with olaparib \pm 4 Gy radiation and measured the total PAR and PARP1 levels in IBC cell lines. In SUM-190 and MDA-IBC-3 cells, PAR formation is significantly inhibited with $1\mu\text{M}$ of olaparib (Fig. 4B,C). The same effect is seen in SUM-149 cells after treatment with $1\mu\text{M}$ olaparib (Supplemental Fig. 2). Inhibition of PAR formation, however, can also be achieved at the same level in SUM-149 cells with 20nM of olaparib (Fig. 4D). Therefore, inhibition of PAR formation with olaparib occurs at low concentrations (20nM) that are sufficient to confer radiosensitization in SUM-149 cells. Though olaparib effectively inhibits PARylation at these concentrations, the amount of PARP1 in the cell lines remains relatively constant in all models (Fig. 4B–D).

PARP1 inhibition significantly inhibits growth of SUM-190 xenografts *in vivo*

Having demonstrated that PARP1 inhibition can effectively radiosensitize IBC cell lines *in vitro*, we next sought to validate these findings in an *in vivo* xenograft model. For *in vivo* studies, subcutaneous tumors were allowed to reach $\sim 80\text{ mm}^3$ in CB-17 SCID mice whereupon treatment was initiated with one of the following: vehicle, 50 mg/kg olaparib alone daily, radiation alone (8 fractions of 2 Gy), or the combination (olaparib 50 mg/kg + 2 Gy RT daily for 8 fractions) (Fig. 5A). To truly assess the radiosensitizing effects of PARP1 inhibition, olaparib treatment was started one day before initiation of radiation and discontinued after the last fraction of radiation. Consistent with the *in vitro* proliferation assays, treatment with olaparib alone did not significantly delay tumor growth or doubling time of xenograft tumors. As expected, radiation alone did lead to a decrease in tumor size initially, but tumors continued to grow after the completion of fractionated radiation (Fig. 5B). Mice receiving both radiation and olaparib treatment had significantly smaller tumors after completion of the study compared to those receiving radiation alone ($p < 0.0001$).

There was a significant delay in the time to tumor doubling ($p < 0.0001$, Fig. 5C) and tripling ($p < 0.0001$, Fig. 5D) in the animals treated with combination olaparib and RT. In addition, time to tumor doubling and tripling was not reached in the combination treated group after 35 days. Weights of the mice (Fig. 5E) remained relatively constant throughout the experiment, indicating there was limited toxicity observed with combination treatment. Interestingly, the effects of the combination treatment with olaparib and radiation were found to be synergistic using the fractional tumor volume (FTV) method as previously described (Fig. 5F)(12). Immunohistochemistry studies in tumors harvested from the mice at the end of the experiment demonstrated that levels of Ki67, a marker of cell proliferation, were significantly decreased in all treatment groups compared to control mice, with the most significant decrease in the combination treated animals ($p = 0.0004$, Supplemental Fig. 3A,B). There was also a decrease in p16 staining levels in the mice treated with radiation alone ($p = 0.0072$) and the combination treated group ($p = 0.0385$) in the long-term experiments (Supplemental Fig. 3C,D), suggesting a decrease in cellular senescence in these tumors(18). The on-target effects of olaparib were confirmed in the short-term studies (48 hours of PARPi treatment alone or 24 hours of PARPi pretreatment before radiation). As expected, total levels of PARP1 were unaffected by treatment with olaparib, radiation, or the combination treatment (Supplemental Fig. 4A,B), while PAR levels were significantly lower in the PARPi treated animals (Supplemental Fig. 4C,D).

Discussion

In this study, we demonstrate that PARP1 inhibition alone is insufficient in delaying IBC cell line growth and proliferation (Fig. 1). Combination treatment with PARP1 inhibition and ionizing radiation, however, results in significant radiosensitization of IBC models *in vitro* (Fig. 2), and the combination treatment results in delayed tumor growth *in vivo* (Fig. 5). Additionally, we demonstrate that PARP1 inhibition in combination with radiation significantly delays resolution of dsDNA breaks using *in vitro* models of IBC (Fig. 3, Fig. 4). Taken together, these results suggest that PARP1 inhibition with radiation therapy may be a promising strategy for the treatment of inflammatory breast cancer. Although these studies suggest that PARP1 inhibition may be an effective radiosensitization strategy for the treatment of IBC, other potential targets for treatment have also been identified. Several groups have identified molecular alterations in IBC tumors and *in vitro* models that may help to describe the aggressive phenotype associated with IBC(1). Owing to the inflammatory nature of these cancers, the use of lipid lowering agents like statins has been met with some success(19,20). Preclinical data using statins in IBC show statin treatment can lead to increased apoptosis and radiosensitivity, inhibition of proliferation and invasion, and decreased metastatic dissemination of tumors(21). In a population-based cohort study in patients with IBC, statin use was associated with improved progression-free survival in IBC patients(21). Recent studies have sought to better define this inflammatory microenvironment, and many have noted that macrophages may be important in mediating the radiosensitivity and metastatic potential of IBC tumors(22–25). Immune regulating agents have also been implicated in the aggressiveness of IBC. In addition to the role that cytokines like INF α and TNF α may play in pathogenesis(26), many studies have reported that PD-L1 is consistently overexpressed in IBC tumors(27,28). Upregulation of downstream

effective strategy for women with IBC (and in women with locoregionally recurrent breast cancer)(50). To that end, a randomized phase II trial (SWOG 1706,) comparing the effects of olaparib and radiation therapy to radiation therapy alone in patients with IBC is now underway. Patients in the combination arm begin treatment with olaparib one day prior to the initiation of radiation therapy, and olaparib is administered until the final day of radiation treatment. Invasive disease-free survival of women receiving treatment with olaparib and radiation will be compared to that of the group receiving radiation alone. Secondary endpoints, like local disease control, distant relapse-free survival and overall survival will also be assessed. In addition, correlative studies from this trial will be used to see if biomarkers of treatment response and efficacy can be identified. These correlative studies will also define the genomic and transcriptomic landscape of IBC in a large patient population and will assess how circulating tumor DNA (ctDNA) levels are affected by combination and single agent treatment. Though it is evident from our study that PARP1 inhibition with olaparib leads to radiosensitization of IBC cell lines, further studies are needed to determine the exact mechanism of olaparib-induced radiosensitization in IBC. Future transcriptomic and proteomic analysis of current model systems across multiple platforms may provide some insight as to the mechanism of this radiosensitization, and such studies are currently underway. Finally, correlative studies from SWOG 1706 will help inform future mechanistic studies and will provide a platform in which to evaluate potential predictive or prognostic biomarkers that may be able to help more effectively guide selection of IBC patients for this approach to treatment intensification.

Supplementary Material

Refer to Web version on PubMed Central for supplementary material.

Acknowledgments:

The Breast Cancer Research Foundation (N026000 to L. Pierce), The Komen for the Cure Foundation (N053349 to R. Jaggi), the University of Michigan Rogel Cancer Center (P30CA046592 to C. Speers). A. Michmerhuizen, A. Pesch and B. Chandler are all supported by training grants through the National Institute of Health. A. Michmerhuizen is supported by T32-GM007315 (NIGMS), A. Pesch is supported by T32-GM007767 (NIGMS), and B. Chandler is supported by T32-CA140044 (NCI). Wendy Woodward at MD Anderson Cancer Center for providing MDA-IBC-3 cells, and Stephen Ethier at the Medical University of South Carolina for providing SUM-149 and SUM-190 cells.

References

1. Menta A, Fouad TM, Lucci A, Le-Petross H, Stauder MC, Woodward WA, et al. Inflammatory Breast Cancer: What to Know About This Unique, Aggressive Breast Cancer. *Surg Clin North Am* 2018;98:787–800. [PubMed: 30005774]
2. Li J, Xia Y, Wu Q, Zhu S, Chen C, Yang W, et al. Outcomes of patients with inflammatory breast cancer by hormone receptor-and HER2-defined molecular subtypes: A population-based study from the SEER program. *Oncotarget*. 2017;8:49370. [PubMed: 28472761]
3. Ross JS, Ali SM, Wang K, Khaira D, Palma NA, Chmielecki J, et al. Comprehensive genomic profiling of inflammatory breast cancer cases reveals a high frequency of clinically relevant genomic alterations. *Breast Cancer Res Treat* 2015;154:155–62. [PubMed: 26458824]
4. Wedam SB, Low JA, Yang SX, Chow CK, Choyke P, Danforth D, et al. Antiangiogenic and antitumor effects of bevacizumab in patients with inflammatory and locally advanced breast cancer. *J Clin Oncol* 2006;24:769–77. [PubMed: 16391297]

5. Yang SX, Steinberg SM, Nguyen D, Wu TD, Modrusan Z, Swain SM. Gene expression profile and angiogenic marker correlates with response to neoadjuvant bevacizumab followed by bevacizumab plus chemotherapy in breast cancer. *Clin Cancer Res* 2008;14:5893–9. [PubMed: 18794102]
6. Bourcier C, Pessoa EL, Dunant A, Heymann S, Spielmann M, Uzan C, et al. Exclusive alternating chemotherapy and radiotherapy in nonmetastatic inflammatory breast cancer: 20 years of follow-up. *Int J Radiat Oncol Biol Phys* 2012;82:690–5. [PubMed: 21277101]
7. Gelmon KA, Tischkowitz M, Mackay H, Swenerton K, Robidoux A, Tonkin K, et al. Olaparib in patients with recurrent high-grade serous or poorly differentiated ovarian carcinoma or triple-negative breast cancer: a phase 2, multicentre, open-label, non-randomised study. *Lancet Oncol* 2011;12:852–61. [PubMed: 21862407]
8. Dent RA, Lindeman GJ, Clemons M, Wildiers H, Chan A, McCarthy NJ, et al. Phase I trial of the oral PARP inhibitor olaparib in combination with paclitaxel for first- or second-line treatment of patients with metastatic triple-negative breast cancer. *Breast Cancer Res* 2013;15:R88. [PubMed: 24063698]
9. Comen EA, Robson M. Poly(ADP-Ribose) Polymerase Inhibitors in Triple-Negative Breast Cancer. *Cancer J* 2010;16:48–52. [PubMed: 20164690]
10. Feng FY, Speers C, Liu M, Jackson WC, Moon D, Rinkinen J, et al. Targeted radiosensitization with PARP1 inhibition: optimization of therapy and identification of biomarkers of response in breast cancer. *Breast Cancer Res Treat* 2014;147:81–94. [PubMed: 25104443]
11. Speers C, Zhao SG, Kothari V, Santola A, Liu M, Wilder-Romans K, et al. Maternal Embryonic Leucine Zipper Kinase (MELK) as a Novel Mediator and Biomarker of Radioresistance in Human Breast Cancer. *Clin Cancer Res* 2016;22:5864–75. [PubMed: 27225691]
12. Matar P, Rojo F, Cassia R, Moreno-Bueno G, Di Cosimo S, Tabernero J, et al. Combined epidermal growth factor receptor targeting with the tyrosine kinase inhibitor gefitinib (ZD1839) and the monoclonal antibody cetuximab (IMC-C225): superiority over single-agent receptor targeting. *Clin Cancer Res* 2004;10:6487–501. [PubMed: 15475436]
13. Yokoyama Y, Dhanabal M, Griffioen AW, Sukhatme VP, Ramakrishnan S. Synergy between angiostatin and endostatin: inhibition of ovarian cancer growth. *Cancer Res* 2000;60:2190–6. [PubMed: 10786683]
14. Donawho CK, Luo Y, Penning TD, Bauch JL, Bouska JJ, Bontcheva-Diaz VD, et al. ABT-888, an orally active poly(ADP-ribose) polymerase inhibitor that potentiates DNA-damaging agents in preclinical tumor models. *Clin Cancer Res* 2007;13:2728–37. [PubMed: 17473206]
15. Elstrodt F, Hollestelle A, Nagel JH, Gorin M, Wasielewski M, van den Ouweland A, et al. BRCA1 mutation analysis of 41 human breast cancer cell lines reveals three new deleterious mutants. *Cancer Res* 2006;66:41–5. [PubMed: 16397213]
16. Skov K, Macphail S. Interaction of platinum drugs with clinically relevant x-ray doses in mammalian cells: a comparison of cisplatin, carboplatin, iproplatin, and tetraplatin. *Int J Radiat Oncol* 1991;20:221–5.
17. Zhang X, Yang H, Gu K, Chen J, Rui M, Jiang G-L. In vitro and in vivo study of a nanoliposomal cisplatin as a radiosensitizer. *Int J Nanomedicine* 2011;6:437. [PubMed: 21499433]
18. Althubiti M, Lezina L, Carrera S, Jukes-Jones R, Giblett SM, Antonov A, et al. Characterization of novel markers of senescence and their prognostic potential in cancer. *Cell Death Dis* 2014;5:1528.
19. Wolfe AR, Debeb BG, Lacerda L, Larson R, Bambhroliya A, Huang X, et al. Simvastatin prevents triple-negative breast cancer metastasis in pre-clinical models through regulation of FOXO3a. *Breast Cancer Res Treat* 2015;154:495–508. [PubMed: 26590814]
20. Van Wyhe RD, Rahal OM, Woodward WA. Effect of statins on breast cancer recurrence and mortality: a review. *Breast Cancer* 2017;9:559–65. [PubMed: 29238220]
21. Brewer TM, Masuda H, Liu DD, Shen Y, Liu P, Iwamoto T, et al. Statin use in primary inflammatory breast cancer: a cohort study. *Brit J Cancer* 2013;109:318. [PubMed: 23820253]
22. Reddy JP, Atkinson RL, Larson R, Burks JK, Smith D, Debeb BG, et al. Mammary stem cell and macrophage markers are enriched in normal tissue adjacent to inflammatory breast cancer. *Breast Cancer Res Treat* 2018;171:283–93. [PubMed: 29858753]

23. Allen SG, Chen Y-C, Madden JM, Fournier CL, Altemus MA, Hiziroglu AB, et al. Macrophages enhance migration in inflammatory breast cancer cells via RhoC GTPase signaling. *Sci Rep* 2016;6:39190. [PubMed: 27991524]
24. Rahal OM, Wolfe AR, Mandal PK, Larson R, Tin S, Jimenez C, et al. Blocking Interleukin (IL)4- and IL13-Mediated Phosphorylation of STAT6 (Tyr641) Decreases M2 Polarization of Macrophages and Protects Against Macrophage-Mediated Radioresistance of Inflammatory Breast Cancer. *Int J Radiat Oncol Biol Phys* 2018;100:1034–43. [PubMed: 29485045]
25. Wolfe AR, Trenton NJ, Debeb BG, Larson R, Ruffell B, Chu K, et al. Mesenchymal stem cells and macrophages interact through IL-6 to promote inflammatory breast cancer in pre-clinical models. *Oncotarget* 2016;7:82482–92. [PubMed: 27756885]
26. Bertucci F, Finetti P, Vermeulen P, Van Dam P, Dirix L, Birnbaum D, et al. Genomic Profiling of Inflammatory Breast Cancer: A Review. *Breast* 2014;23:538–45. [PubMed: 24998451]
27. Bertucci F, Finetti P, Colpaert C, Mamessier E, Parizel M, Dirix L, et al. PDL1 expression in inflammatory breast cancer is frequent and predicts for the pathological response to chemotherapy. *Oncotarget* 2015;6:13506–19. [PubMed: 25940795]
28. Hamm CA, Moran D, Rao K, Trusk PB, Pry K, Sausen M, et al. Genomic and Immunological Tumor Profiling Identifies Targetable Pathways and Extensive CD8+/PDL1+ Immune Infiltration in Inflammatory Breast Cancer Tumors. *Mol Cancer Ther* 2016;15:1746–56. [PubMed: 27196778]
29. Jhaveri K, Teplinsky E, Silvera D, Valeta-Magara A, Arju R, Giashuddin S, et al. Hyperactivated mTOR and JAK2/STAT3 pathways: molecular drivers and potential therapeutic targets of inflammatory and invasive ductal breast cancers after neoadjuvant chemotherapy. *Clin Breast Cancer* 2016;16:113–22. [PubMed: 26774497]
30. Wynn ML, Yates JA, Evans CR, Van Wassenhove LD, Wu ZF, Bridges S, et al. RhoC GTPase is a potent regulator of glutamine metabolism and N-acetylaspartate production in inflammatory breast cancer cells. *J Biol Chem* 2016;291:13715–29. [PubMed: 27129239]
31. Joglekar M, Elbezanti WO, Weitzman MD, Lehman HL, van Golen KL. Caveolin-1 mediates inflammatory breast cancer cell invasion via the Akt1 pathway and RhoC GTPase. *J Cell Biochem* 2015;116:923–33. [PubMed: 25559359]
32. Balamurugan K, Sterneck E. The Many Faces of C/EBP δ and their Relevance for Inflammation and Cancer. *Int J Biol Sci.* 2013;9:917. [PubMed: 24155666]
33. Allensworth JL, Evans MK, Bertucci F, Aldrich AJ, Festa RA, Finetti P, et al. Disulfiram (DSF) acts as a copper ionophore to induce copper-dependent oxidative stress and mediate anti-tumor efficacy in inflammatory breast cancer. *Mol Oncol.* 2015;9:1155–68. [PubMed: 25769405]
34. Arora J, Sauer SJ, Tarpley M, Vermeulen P, Rypens C, Van Laere S, Williams KP, Devi GR, Dewhirst MW. Inflammatory breast cancer tumor emboli express high levels of anti-apoptotic proteins: use of a quantitative high content and high-throughput 3D IBC spheroid assay to identify targeting strategies. *Oncotarget.* 2017; 8:25848. [PubMed: 28460441]
35. Lerebours F, Vacher S, Andrieu C, Espie M, Marty M, Lidereau R, et al. NF-kappa B genes have a major role in Inflammatory Breast Cancer. *BMC Cancer* 2008;8:41. [PubMed: 18248671]
36. Van Laere SJ, Van der Auwera I, Van den Eynden GG, van Dam P, Van Marck EA, Vermeulen PB, et al. NF- κ B activation in inflammatory breast cancer is associated with oestrogen receptor downregulation, secondary to EGFR and/or ErbB2 overexpression and MAPK hyperactivation. *Brit J Cancer* 2007;97:659. [PubMed: 17700572]
37. Murai J, Huang Sy N, Das BB, Renaud A, Zhang Y, Doroshow JH, et al. Differential trapping of PARP1 and PARP2 by clinical PARP inhibitors. *Cancer Res* 2012;72:5588–99. [PubMed: 23118055]
38. Menear KA, Adcock C, Boulter R, Cockcroft XL, Copsey L, Cranston A, et al. 4-[3-(4-cyclopropanecarbonylpiperazine-1-carbonyl)-4-fluorobenzyl]-2H-phthalazin-1-one: a novel bioavailable inhibitor of poly(ADP-ribose) polymerase-1. *J Med Chem* 2008;51:6581–91. [PubMed: 18800822]
39. Parsels LA, Karnak D, Parsels JD, Zhang Q, Velez-Padilla J, Reichert ZR, et al. PARP1 Trapping and DNA Replication Stress Enhance Radiosensitization with Combined WEE1 and PARP Inhibitors. *Mol Cancer Res* 2018;16:222–32. [PubMed: 29133592]

40. Murai J, Zhang Y, Morris J, Ji J, Takeda S, Doroshow JH, et al. Rationale for Poly(ADP-ribose) Polymerase (PARP) Inhibitors in Combination Therapy with Camptothecins or Temozolomide Based on PARP Trapping versus Catalytic Inhibition. *J Pharmacol Exp Ther* 2014;349:408–16. [PubMed: 24650937]
41. Maya-Mendoza A, Moudry P, Merchut-Maya JM, Lee M, Strauss R, Bartek J. High speed of fork progression induces DNA replication stress and genomic instability. *Nature* 2018;559:279–84. [PubMed: 29950726]
42. Drew Y, Ledermann J, Hall G, Rea D, Glasspool R, Highley M, et al. Phase 2 multicentre trial investigating intermittent and continuous dosing schedules of the poly(ADP-ribose) polymerase inhibitor rucaparib in germline BRCA mutation carriers with advanced ovarian and breast cancer. *Brit J Cancer* 2016;114:723–30. [PubMed: 27002934]
43. Litton JK, Rugo HS, Ettl J, Hurvitz SA, Goncalves A, Lee KH, et al. Talazoparib in Patients with Advanced Breast Cancer and a Germline BRCA Mutation. *N Engl J Med* 2018;379:753–63. [PubMed: 30110579]
44. Karam SD, Reddy K, Blatchford PJ, Waxweiler T, DeLouize AM, Oweida A, et al. Final Report of a Phase I Trial of Olaparib with Cetuximab and Radiation for Heavy Smoker Patients with Locally Advanced Head and Neck Cancer. *Clin Cancer Res* 2018;24:4949–59. [PubMed: 30084837]
45. Vance S, Liu E, Zhao L, Parsels JD, Parsels LA, Brown JL, et al. Selective radiosensitization of p53 mutant pancreatic cancer cells by combined inhibition of Chk1 and PARP1. *Cell Cycle* 2011;10:4321–9. [PubMed: 22134241]
46. Han S, Brenner JC, Sabolch A, Jackson W, Speers C, Wilder-Romans K, et al. Targeted radiosensitization of ETS fusion-positive prostate cancer through PARP1 inhibition. *Neoplasia* 2013;15:1207–17. [PubMed: 24204199]
47. Bi Y, Verginadis II, Dey S, Lin L, Guo L, Zheng Y, et al. Radiosensitization by the PARP inhibitor olaparib in BRCA1-proficient and deficient high-grade serous ovarian carcinomas. *Gynecol Oncol* 2018;150:534–44. [PubMed: 30025822]
48. Wurster S, Hennes F, Parpys AC, Seelbach JI, Mansour WY, Zielinski A, et al. PARP1 inhibition radiosensitizes HNSCC cells deficient in homologous recombination by disabling the DNA replication fork elongation response. *Oncotarget* 2016;7:9732–41. [PubMed: 26799421]
49. Mangoni M, Sottili M, Salvatore G, Meattini I, Desideri I, Greto D, et al. Enhancement of Soft Tissue Sarcoma Cell Radiosensitivity by Poly(ADP-ribose) Polymerase-1 Inhibitors. *Radiat Res* 2018;190:464–72. [PubMed: 30067444]
50. Jagsi R, Griffith K, Bellon J, Woodward W, Horton J, Ho A, et al. TBCRC 024 initial results: A multicenter phase 1 study of veliparib administered concurrently with chest wall and nodal radiation therapy in patients with inflammatory or locoregionally recurrent breast cancer. *Int J Radiat Onc* 2015;93:S137.

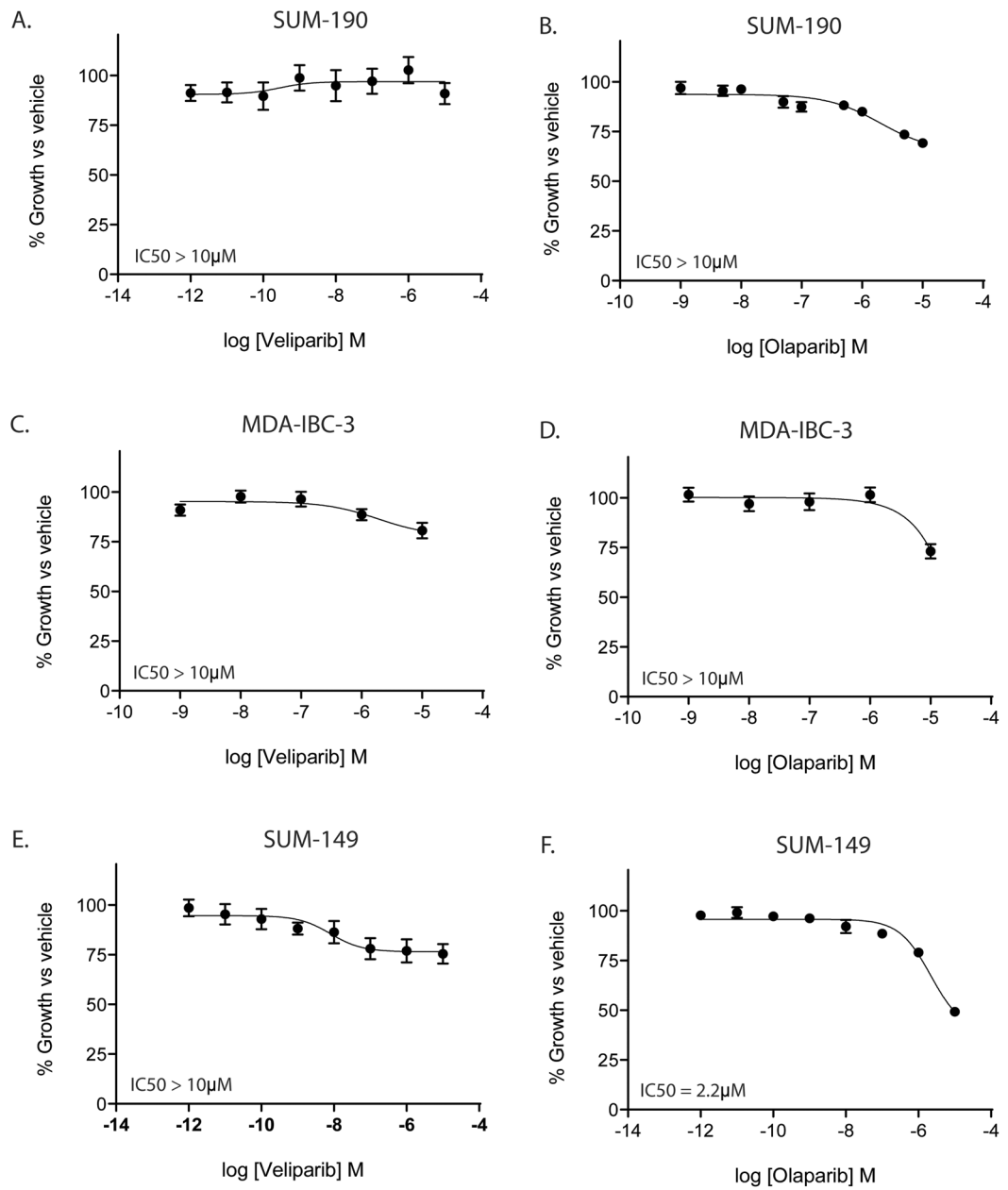


Figure 1: PARP1 inhibition does not affect proliferation of IBC cell lines.

IBC cell lines were treated with either olaparib or veliparib and cell viability was measured 72 hours after treatment. In SUM-190 (A,B) and MDA-IBC-3 (C,D) cells, neither veliparib or olaparib showed significant effects on proliferation at doses up to 10µM. In SUM-149 cells (E,F), olaparib, but not veliparib, can inhibit proliferation at high doses (2.2µM). Graphs are shown as the average of three independent experiments ± SEM.

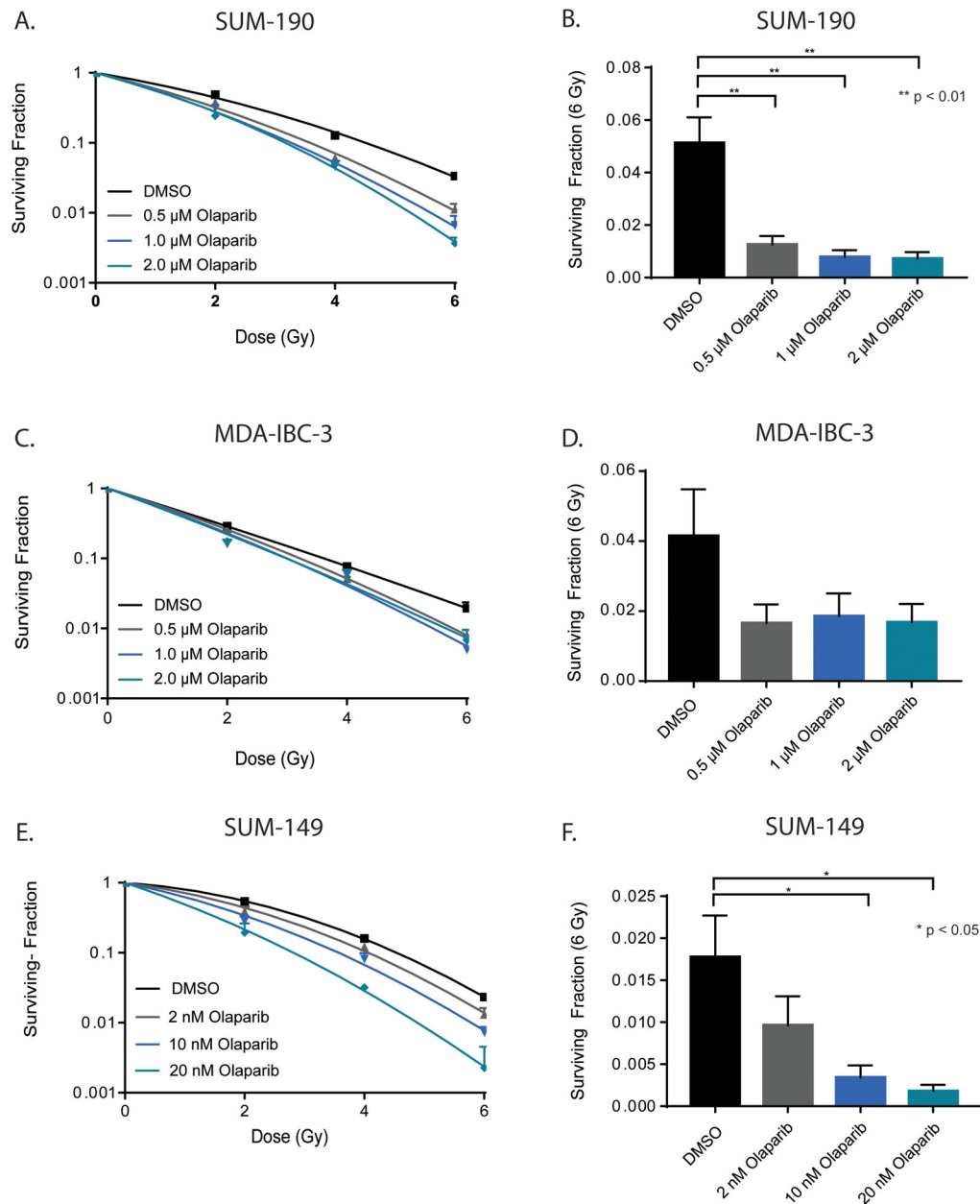


Figure 2: Clonogenic survival of IBC cell lines decreases with olaparib treatment. Olaparib treatment results in a dose-dependent reduction in survival fraction of SUM-190 (A), MDA-IBC-3 (C), and SUM-149 (E) cell lines. Representative data from single experiments are shown for each cell line. The surviving fraction of cells after 6 Gy (B, D, F) was calculated as the mean of three independent experiments and depicted \pm SEM for each cell line. ($p < 0.05 = *$, $p < 0.01 = **$)

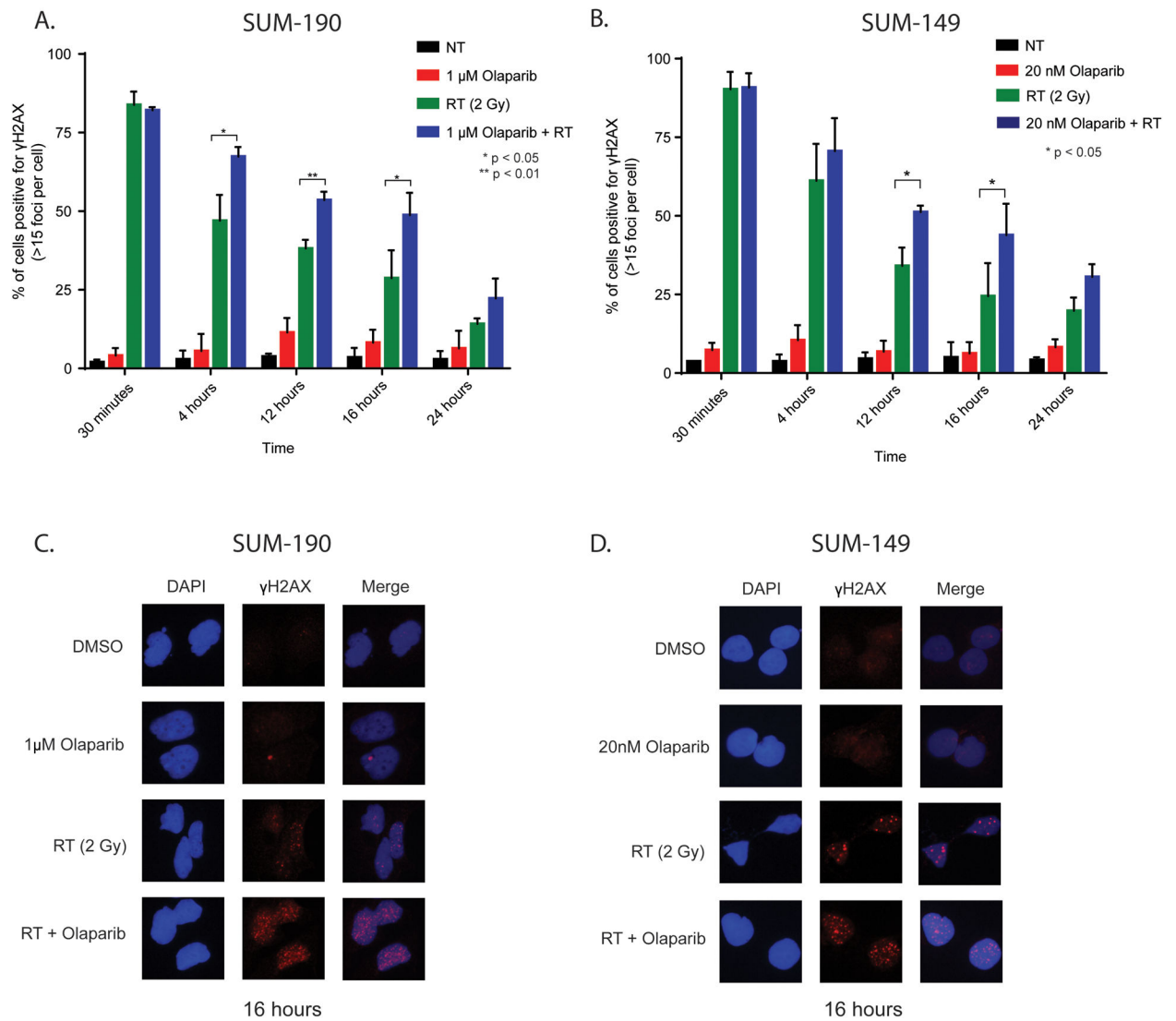


Figure 3: Radiation in combination with the PARP1 inhibition leads to persistence of DNA damage in IBC cell lines.

Immunofluorescence microscopy was used to measure γ H2AX foci in SUM-190 (A) and SUM-149 (B) cells. Cells were pretreated for one hour with olaparib and fixed at 0.5, 4, 12, 16, and 24 hours after radiation, then stained for DAPI and γ H2AX. Cells containing 15 foci were scored as positive. In SUM-190 cells at 4, 12, and 16 hours, there were significantly higher levels of cells positive for γ H2AX for those treated with the combination of 2 Gy radiation and 1 μ M olaparib compared to cells treated with 2 Gy radiation alone. In SUM-149 cells, 20 nM olaparib and 2 Gy radiation results in a higher percentage of γ H2AX positive cells compared to cells treated with radiation alone at both 12 and 16 hours. Representative images of γ H2AX foci in SUM-190 (C) and SUM-149 (D) cells at 16 hours are shown for all treatment groups. Graphs represent the average of three independent experiments \pm SD. ($p < 0.05 = *$)

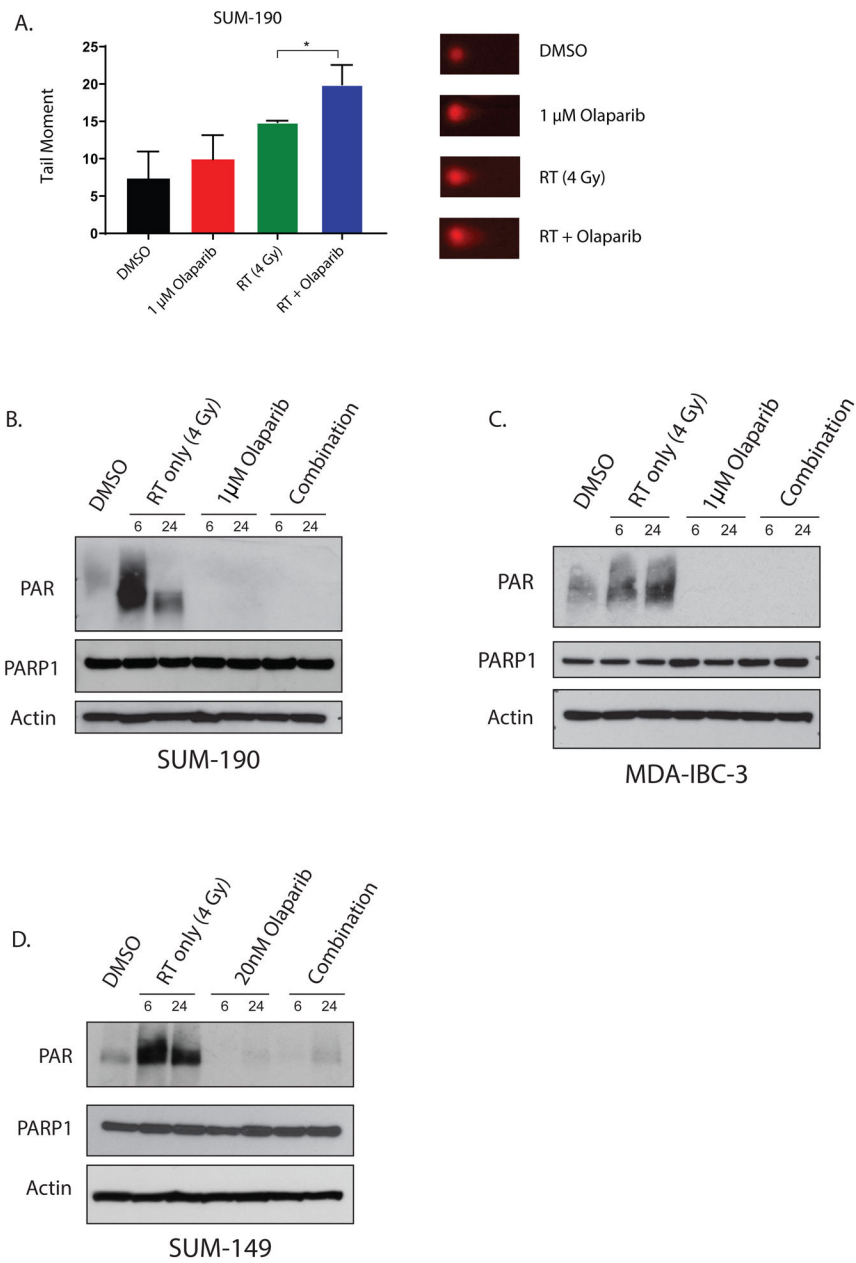


Figure 4: PARP1 inhibition increases dsDNA breaks and significantly decreases PAR formation in IBC cell lines.

Neutral comet assay in SUM-190 cells (**A**) shows higher levels of dsDNA damage at 4 hours in cells treated with radiation and olaparib compared to untreated cells, or cells treated with RT or olaparib alone ($p < 0.05 = *$). Graphs represent the average of three independent experiments \pm SD and representative images for each treatment are shown. In SUM-190 (**B**) and MDA-IBC-3 (**C**) cells, radiation induced DNA damage causes an increase in PAR formation at both 6 and 24 hours after 4 Gy radiation. In the combination group that receives a one-hour pretreatment of 1 μ M olaparib before radiation, PAR formation is significantly lower at 6 and 24 hours after RT. In SUM-149 (**D**) cells, this same trend can be observed at a much lower dose of olaparib (20nM). Though the enzymatic activity of PARP1 is efficiently

inhibited at these doses, total levels of PARP are not significantly different across the treatment conditions.

Author Manuscript

Author Manuscript

Author Manuscript

Author Manuscript

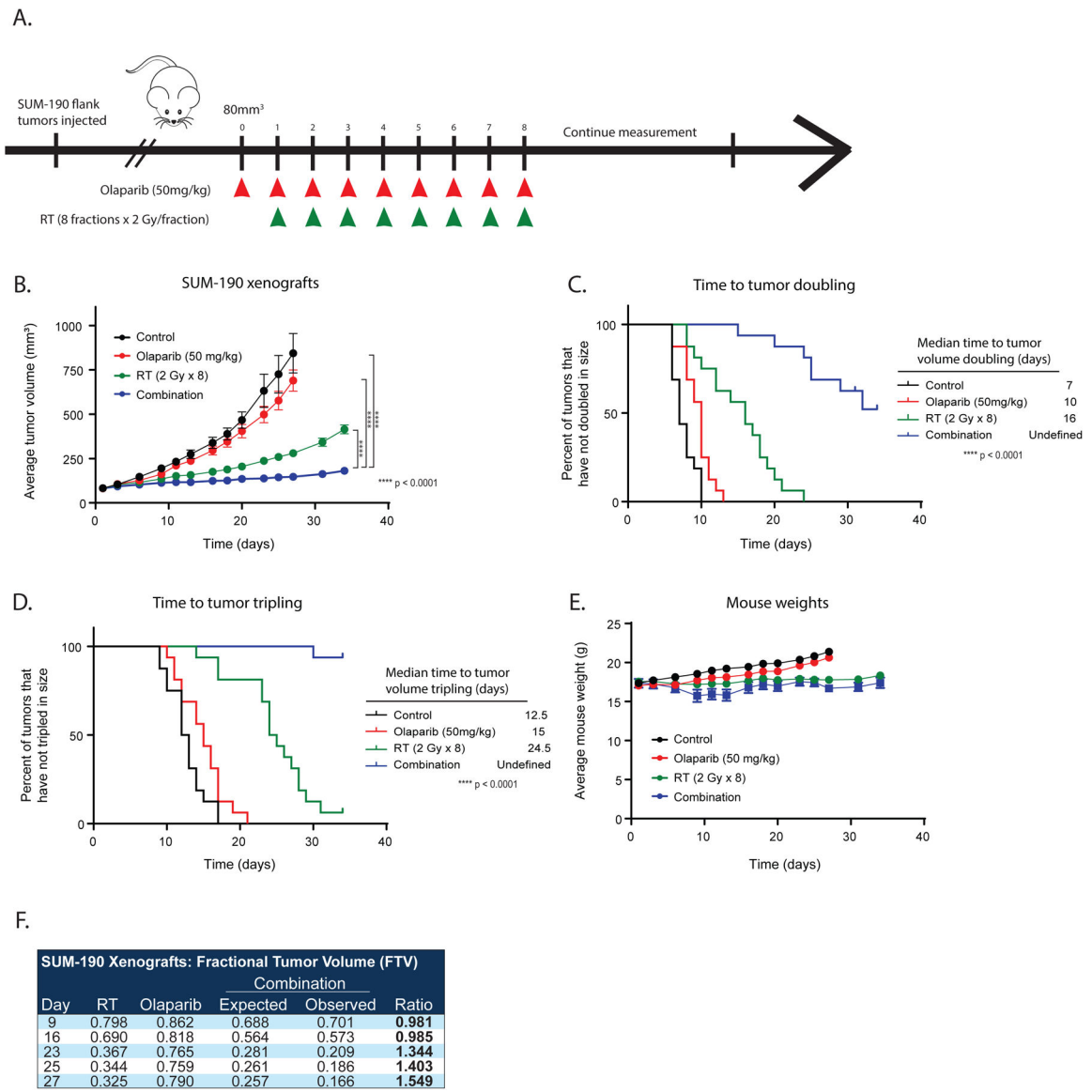


Figure 5: PARP1 inhibition with radiation is more effective than radiation alone in a SUM-190 xenograft model.

SUM-190 cells were subcutaneously injected into CB17-SCID mice, and treatment was started when tumors reached approximately 80 mm³ (A). Olaparib treatment began one day before the initiation of radiation treatment and ended on the same day as the last fraction of radiation. With this paradigm, the combination treatment leads to delayed growth of tumors (B) and an increased time to tumor doubling (C) and tumor tripling (D) (p < 0.0001 = ****). The treatment did not display significant toxicities, and animal weights were not significantly different between the treatment groups (E). Using the FTV method, there was a synergistic effect with olaparib and RT treatment to antagonize tumor growth (ratios >1 indicate synergism) (F). A two-way ANOVA was performed to compare tumor volume between experimental groups.